Journal of Fluids and Structures (1998) **12,** 1055–1071
Article No. fl980182

AN EFFICIENT LIQUID SLOSHING DAMPER FOR VIBRATION CONTROL

V. J. Modi and S. R. Munshi

Department of Mechanical Engineering, The University of British Columbia Vancouver, British Columbia, Canada V6T 1Z4

(Received 10 March 1998 and in revised form 31 July 1998)

The next generation of tall structures are being designed to be lighter and more flxible, making them susceptible to wind, ocean waves and earthquake type of excitations. One approach to vibration control of such systems is through energy dissipation using a liquid sloshing damper. Such dampers are already in use for vibration control of tall structures in Japan and Australia. The present parametric study focuses on enhancing the energy dissipation efficiency of a rectangular liquid damper through introduction of a two-dimensional obstacle. A parametric free-vibration study, aimed at optimum size and location of the obstacle, is described first. Results suggest a significant increase in the energy dissipation, up to 60%, in the presence of the obstacle. An extensive wind tunnel test-program was undertaken which substantiated the effectiveness of the improved damper in suppressing both vortex resonance and galloping types of instabilities. Ability of the damper to control structural oscillations with a smaller amount liquid is quite attractive for real-life applications.

1. INTRODUCTION

A flexible structure could experience dynamic motion due to a variety of cases. In case of ground- and ocean-based structures the excitation is in the form of a single or combination of physical causes, such as wind, ocean waves/currents and earthquakes. The resulting structural motion could be due to fluid–structure interaction instabilities (e.g. vortex-induced vibrations, galloping motion, flutter and turbulence-induced buffeting) or wave-induced motions (e.g. heave, surge, pitch, etc.) of the structure. It should be noted that such excitations could be narrow-band periodic or random in nature. In case of earth-quake, the structure experiences irregular base-excitation. There are also significant differences in the spectral content of the excitation signals among these sources. For example, at frequencies below 1 Hz, the wind-induced loading dominates, whereas in the range 1–10 Hz, the earthquake type of loading is stronger (Kwok 1991). The response is primarily in the first mode, where most of the vibrational energy is stored. Usually it is necessary to keep the structural response within a specified limit. For example, the national building code of Canada suggests a limiting acceleration of 10–30 milli-g's (1 milli-g = 9·81 mm/s^2) for a 10 year return period (Irwin, Ferraro & Stone 1988). It is also known that acceleration below 1 milli-g is not perceptible, whereas acceleration of 10 milli-g or higher is strongly perceptible.

A wide variety of active/passive vibration control systems have been proposed and used in practice. Broadly speaking, they can be classified into two categories: aerodynamic devices to reduce excitation forces, and dampers to dissipate energy.

1.1. Aerodynamic Means of Vibration Suppression

This class of vibration control devices modify the geometry of the structure in such a way as to interfere or weaken the fluid dynamic force responsible for the excitation. Helical strakes,

0889–9746/98/081055 + 17 $30.00

shrouds, slats, fairings, splitter plates, flags, moving surface boundary-layer control, etc. are well known examples (Zdravkovich 1981; Modi, Welt & Seto 1995; Munshi, Modi & Yokomizo, 1996). It should be noted that most of these devices often increase the drag by a significant amount. Furthermore, there are conditions where the suppression of vortex-induced vibration using the aerodynamic reconfiguration is not possible, as in the case of structures with very low damping, or for rows of stacks, as discussed by Ruschweyeh (1980). In general, these devices have not proved successful when applied to offshore structures undergoing wave-excited motions.

1.2. Energy Dissipation Devices

Here the total damping of a structure is increased by introducing some mechanism for energy dissipation. Devices such as a tuned mass damper (TMD), those introducing friction, and tendon-type systems are well-known examples (Hirsch 1980). In recent years, significant progress has taken place in the area of active structural control (Seto 1992). The familiar TMD has evolved into an active version variety, known variously as ATMD (active tuned mass damper), TAD (tuned active damper), AMD (active mass damper), and HDA (hybrid dynamic absorber). In such systems the moving mass could be a simple sliding block of steel or concrete, a semi-circular thick plate rolling back and forth and driven by servo motors (Seto 1992), or a multistage pendulum (Abiru *et al*. 1992). The frequency of the moving mass is closely tuned to the natural frequency of the structure. Most of the active systems operate on the principle of feedback control based on a certain control algorithm. The counter-electromotive force of the servomotor acts as a damping mechanism. Such a system is hybrid in the sense that, in case of a power failure, the moving mass operates as a passive TMD. An active system using the gyroscopic moment of a spinning rotor for stability has also been proposed by Kazao, Takahara, Yamada & Sakamoto (1992). In such a system, each gyro is supported in a single gimbal driven by a servo motor. A couple of gyros are needed for overall control of the structure. A significant increase in the damping, from about 1% to 8%, has been achieved.

A conventional TMD is generally tuned to a single frequency. To overcome this limitation, the MTMD (multiple tuned mass damper) system has been proposed (Fujino & Abe 1992). The MTMD consists of an array of small TMDs whose natural frequencies are distributed over a certain bandwidth. The advantage is that the MTMD is insensitive to mistuning and errors in damping estimation. The damping required for each TMD is smaller, but the amplitude of TMD motion is larger compared to a STMD (single tuned mass damper) system.

A liquid sloshing damper (also known as nutation damper or tuned liquid damper) operates on the principle of energy dissipation through liquid sloshing and wave breaking of the free surface. The device consists of a suitably shaped container partially filled with a liquid (e.g. water). When such a system is subjected to acceleration, the liquid is set into sloshing motion, accompanied by waves at the free surface. Such a device, in a sense, is similar to a MTMD because of its effectiveness over a range of frequencies.

1.3. Liquid Sloshing Dampers

The liquid sloshing damper can have a wide variety of geometries, from toroidal ring to rectangular or circular shaped containers. Furthermore, it may carry internal devices in the form of baffles, screens, moving spheres, particle suspension, etc., interacting with the sloshing motion. Such dampers are ideally suited for suppressing relatively low-frequency motion. They have been in use for quite some time in controlling the librational motion of

satellites (Schneider & Likins 1973; Alfriend & Spencer 1981), where the period may range from 90 min to 24 h. The microgravity environment in space dictates the nutation damper to be completely filled (no free surface). The dissipative wake of a rolling sphere provides damping. As the fundamental frequency of bluff geometries encountered in industrial aerodynamic systems is usually less than 1 Hz, Modi *et al.* decided to apply the concept to this class of problems (Banning, Hengeveld & Modi 1966; Modi, Sun, Shupe & Solyomvari 1981). Subsequently, Modi & Welt (1985) and Welt & Modi (1992) as well as Modi & Seto (1995) have carried out systematic investigation of nutation dampers, both experimentally and analytically.

Tamura *et al.* (1988) have reported application of a liquid sloshing damper to control the vibrations of tall towers. The damper was a circular cylinder (diameter 40 cm), partitioned into seven sections, with a liquid height of 2·1 cm in each section. The mass ratio (i.e. the ratio of liquid mass to generalized mass of the structure) was about 1%. The results indicate that the amplitude of the vibration was reduced by about 50%. Similar dampers have been installed at the Haneda and Narita International airports in Tokyo, Japan (Tamura, Kousaka & Modi 1992). In this case it was found that significant improvement in the damping efficiency can be achieved by adding floating particles (hollow plastic tubes, specific weight = 0·8; length = 1 cm; outer diameter = 0·8 cm; and wall thickness = 0·08 cm). The acceleration response of the towers was reduced by about 55%.

Now, considerable effort has been directed towards an empirical expression that can satisfactorily estimate peak acceleration near the top of a building. Based on 43 buildings tested in the wind tunnel as well as theories of random vibration and wind buffeting, the peak acceleration can be expressed, approximately, as $a_p = p_1\ [U^{p_2}/(Mf_n^{p_2-2}\zeta^{0\cdot5})]$. Here p_1, p_2 are constants and M represents the mass of the building. Since the acceleration approximately varies inversely as the square root of the damping (Masciantonio, Isyumov & Petersen 1987; Irwin, Ferraro & Stone 1988), this corresponds to an effective increase of about 4 times the original damping of the structure.

1.4. Present Investigation

The present study focuses on enhancing the energy dissipation efficiency of the liquid sloshing damper, i.e., to increase the total energy dissipated per cycle, per unit mass of the liquid. To this end, a semicircular obstacle is introduced in the damper to accelerate and enhance the liquid sloshing. The study involves the following.

(i) The effect of system parameters (liquid height, h_w; system natural frequency, f_n; initial displacement, θ_0) on the performance characteristics of a rectangular liquid sloshing damper, without any obstacle. These results serve as reference to assess the effect of an obstacle.

(ii) Experiments with a family of semicircular cross-section obstacles, over a range of r/L and d/L (Figure 1), to assess their effectiveness in increasing the damping.

(iii) Dynamic tests in a wind tunnel to evaluate the effectiveness of the improved liquid sloshing damper in suppressing both vortex resonance and galloping type of fluid–structure interaction instabilities.

2. PHYSICS OF LIQUID SLOSHING INSIDE A CONTAINER

This section describes some of the concepts, to help appreciate the mechanics of energy dissipation inside a liquid sloshing damper. The effect of introducing a semicircular obstacle is also described. It should be mentioned that the analysis is based on the assumption of small amplitude wave motion in a shallow liquid ($h_w/\lambda < 0\cdot05$) (Sorensen 1978).

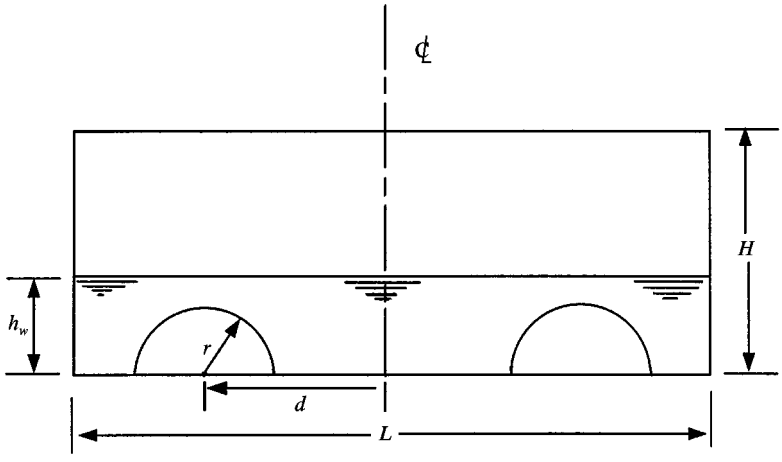

Figure 1. Geometry of the rectangular liquid sloshing damper with obstacles.

2.1. Liquid Frequency

The frequency of small amplitude free surface waves (for the *ij*th mode) in a shallow liquid inside a container with a rectangular geometry [Figure 2(a)] is given by (Blevins 1979)

$$f_{ij} = \frac{1}{2}\sqrt{gh_w}\left[\frac{i^2}{a^2} + \frac{j^2}{b^2}\right]^{1/2}, \quad i, j = 0, 1, 2, \ldots \tag{1}$$

For a container subjected to acceleration in the x-direction, the above expression gives the fundamental liquid frequency as

$$f_l = \frac{1}{2L}\sqrt{gh_w} \quad (i = 1,\ j = 0,\ a = L). \tag{2}$$

2.2. Container Undergoing Angular Vibrations

During free-vibration tests the damper is subjected to angular vibrations. The amplitude of vibration affects the dynamics of liquid motion inside the damper. For small displacements ($\theta_0 \leq 1^\circ$), almost imperceptible surface ripples are observed traveling back and forth inside the damper. There is negligible energy dissipation. For moderate displacements ($1^\circ \leq \theta_0 \leq 2{\cdot}5^\circ$), a single large wave accompanied by small ripples is created. There is a small amount of energy dissipation due to partial breaking of the liquid near the walls of the damper. For large displacement ($\theta_0 \geq 2.5^\circ$), a significant portion of the liquid mass is accelerated. Due to the combined action of large angular motion and high kinetic energy of the accelerated liquid mass, there is considerable sloshing accompanied by overturning of the wave during impact [Figure 2(b)] and breaking of the free surface. This results in much greater energy dissipation.

2.3. Flow Past an Obstacle

Figure 2(c) shows flow past a semi-circular obstacle in a long open channel. From momentum balance considerations for the control volume shown in Figure 2(c), the ratio of

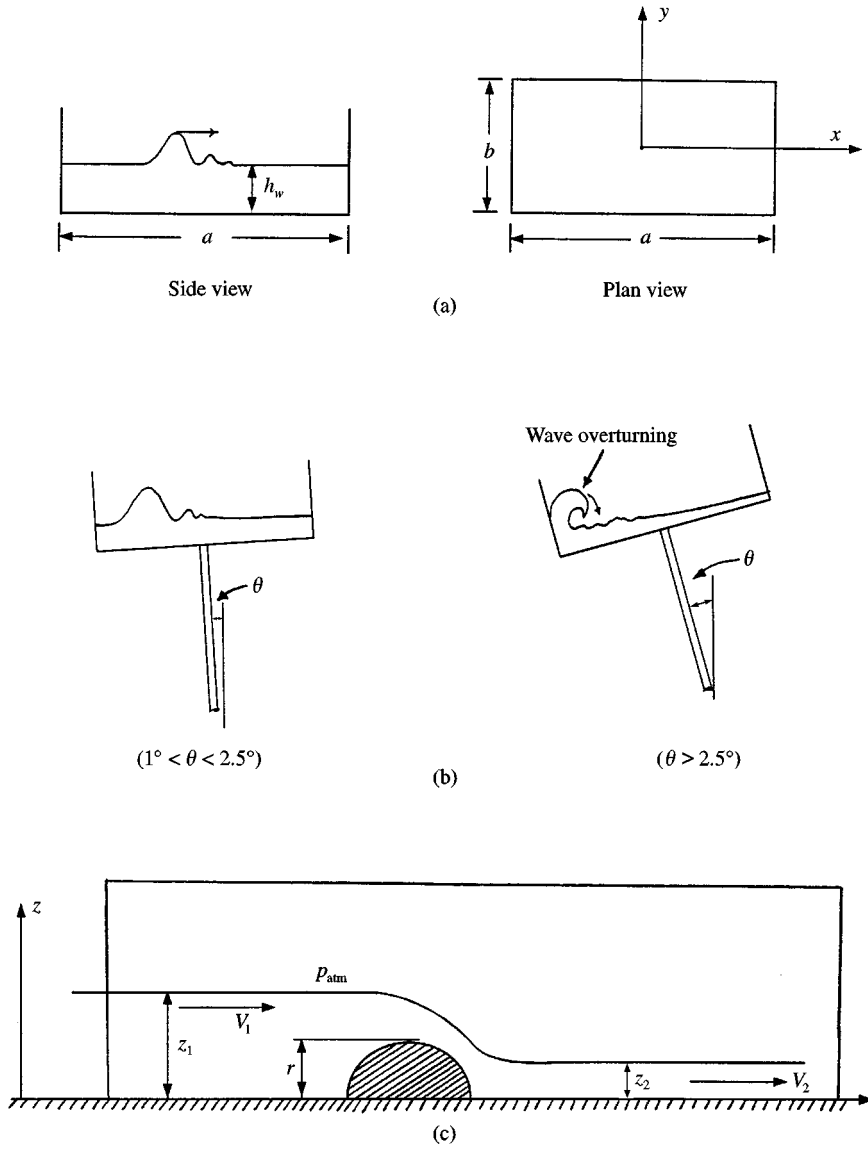

Figure 2. Dynamics of liquid sloshing: (a) liquid sloshing in a rectangular container; (b) liquid damper undergoing angular vibrations; (c) flow past an obstacle.

Froude numbers is given by (Mironer 1979)

$$\frac{F_2}{F_1} = \left(\frac{z_1}{z_2}\right)^{3/2} = \left[\frac{1}{2}(\sqrt{1 + 8F_1^2} - 1)\right]^{-3/2} > 1. \tag{3}$$

The liquid is accelerated while flowing past an obstacle ($V_2 > V_1$). Forbes (1988) has reported an exact nonlinear analysis of this problem.

2.4. Liquid Damper with an Obstacle

In presence of an obstacle, the liquid inside the container is subjected to higher acceleration. The increased kinetic energy of the liquid causes enhanced sloshing, wave overturning and breaking near the damper wall. Overall, the energy dissipation is increased due to the presence of an obstacle. It should be noted that the presence of the container walls do modify the flow past an obstacle (compared to the flow in an infinitely long channel), but the overall behavior is qualitatively similar.

There is an optimum obstacle height (r) for a given liquid height (h_w). For $r \ll h_w$, the free-surface waves are almost unaffected by the presence of the obstacle. For $r \approx h_w$ (r slightly less than h_w), there is a pronounced effect of the obstacle on liquid sloshing. For $r \gg h_w$, the obstacle divides the damper into two separate compartments and as a result loses its significance.

Based on the above background, the following set of experiments were carried out with an aim to develop a liquid damper with higher energy dissipation.

3. FREE VIBRATION EXPERIMENTS

3.1. Test Facility and Calibration

The geometry of the rectangular damper with two-dimensional semicircular cross-section obstacles is shown in Figure 1. The dimensions of the rectangular container are $L = 370$ mm, $W = 166$ mm, and $H = 125$ mm. A semicircular obstacle (radius r) can be placed at a desired location from the axis of symmetry of the damper (distance d). The damper is partially filled with liquid (water) to a desired height (h_w).

A schematic of the vibration test-facility is shown in Figure 3. It consists of a heavy-steel frame support structure. A vertical rod with a bearing is fixed to the support structure as shown in the Figure 3. The rod carries a platform at the top which supports the damper. The natural frequency of the system can be adjusted by locating a set of springs at a desired height. The displacement of the rod is measured by a strain-guaged beam connected through a link. The strain-guage output is processed by a signal conditioning and amplification system and is then sent to a spectrum analyzer and a computer. During some experiments the mass of the liquid was varied. Here the system mass was kept constant by adjusting the auxiliary mass units thus maintaining a constant f_n. The behaviour of the springs and the strain-guaged beam was found to be linear over a range of displacements of 0–100 mm. The overall system accuracy (in terms of frequency and amplitude of the vibration) was within 2%.

3.2. Energy Dissipation Factor

The damping factor is defined as

$$\zeta = \frac{1}{2\pi n} \ln\left(\frac{A_0}{A_n}\right),$$

i.e.,

$$\frac{A_o}{A_n} = \mathrm{e}^{2\pi n\zeta}. \tag{4}$$

The initial potential energy stored in the system is $E_o = \frac{1}{2}kA_o^2$, so that

$$\frac{E_0}{E_n} = \left(\frac{A_o}{A_n}\right)^2 = \mathrm{e}^{4\pi n\zeta}. \tag{5}$$

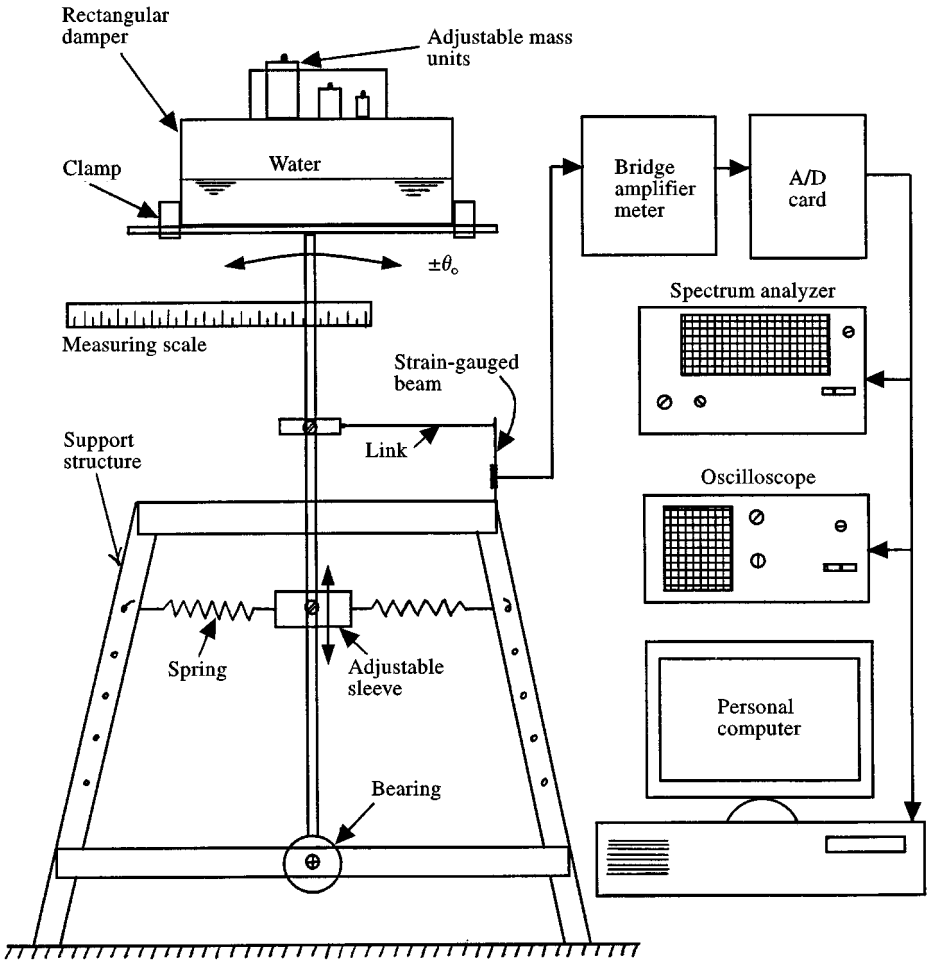

Figure 3. Schematic diagram showing the free vibration set-up used for testing the liquid sloshing dampers.

Thus the average energy dissipation over n cycles is given by

$$\Delta E = \frac{E_o - E_n}{n},$$

i.e.,

$$\Delta E = \frac{E_o}{n}[1 - e^{-4\pi n\zeta}], \tag{6}$$

and the average power dissipated per cycle is

$$\frac{\Delta E}{T} = \frac{E_o f_n}{n}[1 - e^{-4\pi n\zeta}].$$

One can now express the average power dissipated per cycle per unit mass of the liquid as

$$\varepsilon = \frac{E_o f_n}{n m_l}[1 - e^{-4\pi n\zeta}]. \tag{7}$$

3.2. Damper Performance Without an Obstacle

The height of the liquid (h_w) is one of the fundamental parameters governing the behaviour of the damper. In the present study, h_w ranged from 0 to 60 mm ($h_w/L =$ 0 to 0·1622 for $L = 370$ mm). It should be noted that f_l waries as $\sqrt{h_w}$. Figure 4 shows the behaviour of the damper (in terms of ζ and ε) as h_w is varied. The damping factor (ζ) shows a distinct peak near $h_w/L = 0{\cdot}0405$. This corresponds to a resonance ($f_l \approx f_n$) between the liquid frequency and system natural frequency. Figure 4(b) shows the results in terms of energy dissipation per unit mass of liquid. The important thing to note is that now there are two distinct peaks, corresponding to two different values of liquid height, $h_w/L = 0{\cdot}0054$ and 0·0304. The parameter ε is strongly dependent on the liquid mass ($\in \propto m_l^{-1}$, $m_l \propto h_w$), whereas it is relatively weakly dependent ($\varepsilon \propto [1 - \exp(-4\pi n\zeta)]/nh_w \approx 4\pi\zeta/h_w$, for small ζ) on the damping factor (ζ). Hence, at very low liquid height ($h_w/L < 0{\cdot}01$, small m_l), there is a peak in ε. The second peak in ε corresponds to a high ζ. It may be pointed out that for $h_w/L < 0{\cdot}01$, there is hardly any wave motion or liquid sloshing. In fact, the energy dissipation mechanism is more like Coulomb friction between the liquid and the damper walls.

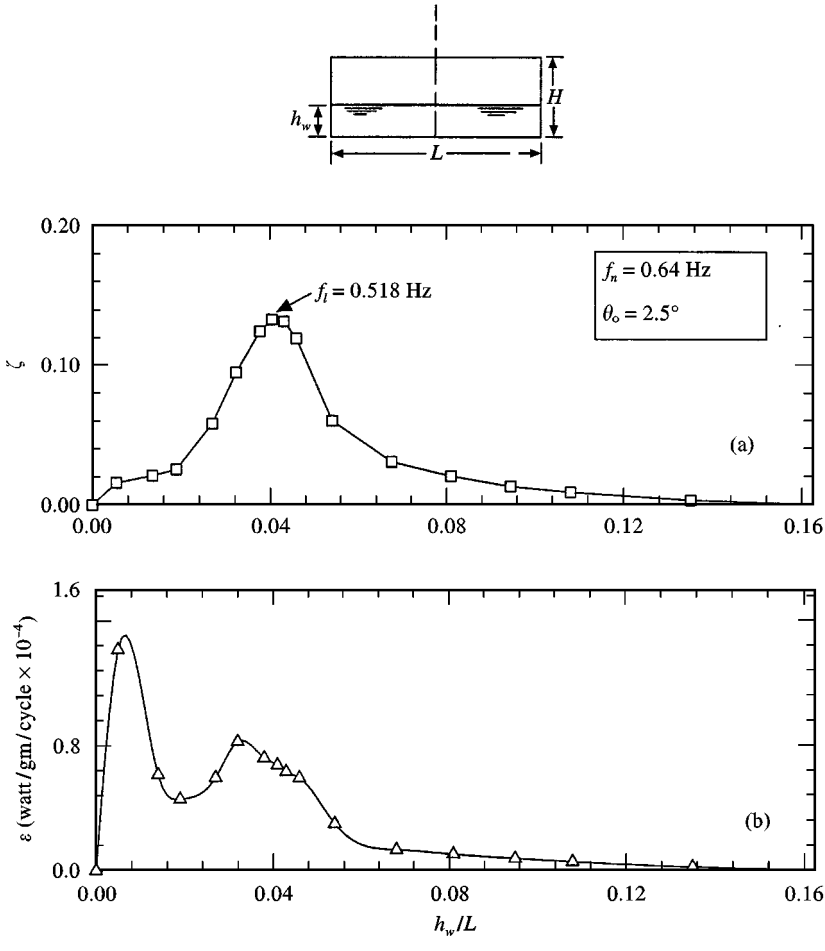

Figure 4. Effect of the liquid height on the performance of the damper.

Thus, it is apparent that a peak in the value of ζ may not correspond to the hightest energy dissipation per unit mass of the liquid. For that purpose ε is an appropriate indicator. Note that, even though ε is highest for $h_w/L = 0{\cdot}0054$, the total energy dissipation is quite small (m_l is small). In practice, such a system would require a large number of dampers, each with a small amount of liquid. On the other hand, one may select the other value of the liquid height, $h_w/L = 0{\cdot}0304$ (corresponding to the second peak), as desirable. Although ε is smaller, the large volume of liquid would result in higher energy dissipation per damper, thus requiring fewer dampers. The final decision would be governed by a variety of factors peculiar to a particular application (space available for storage of dampers, economy of their manufacture, etc.).

The damper performance is also sensitive to the system natural frequency (f_n). In the present set of tests, f_n was varied from 0·16 to 0·8 Hz. During the tests, $h_w = 0{\cdot}0304$ and $\theta_o = 2{\cdot}5°$. Since h_w was fixed, f_l remains constant, but the ratio f_l/f_n varies. Figure 5 shows the variation of ζ and ε with f_l/f_n, where it is noted that there is a peak near $f_l/f_n \approx 1$. There is another, much smaller, yet distinct peak, corresponding to $f_l/f_n \approx 2$, i.e., a superharmonic. Note, the peak is not quite sharp and the damper is effective over a wide range of frequencies.

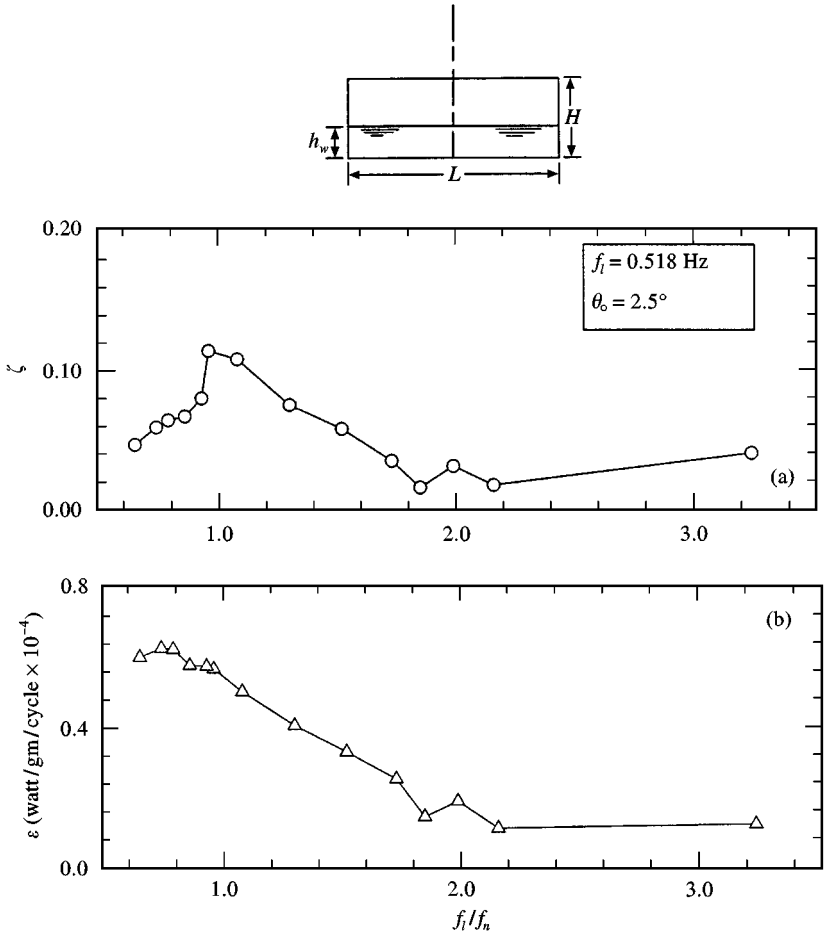

Figure 5. Effect of the natural frequency on the performance of the liquid damper. Note the resonance peak ($f_l \approx f_n$) in the damping factor (ζ).

For a nonlinear vibrating system, the initial displacement is an important parameter. Figure 6 shows the variation of ζ and ε as affected by θ_0. During these tests h_w and f_n remained constant ($h_w/L = 0{\cdot}0304$, $f_n = 0{\cdot}64$ Hz). The initial acceleration imposed upon the liquid is given by $a_0 = \omega_n^2 \theta_o l$. As θ_0 is increased, ζ also increases [Figure 6(a)]. The initial potential energy stored in the system (E_o) also increases with θ_o. However, for large displacements ($\theta_o > 7^\circ$), ζ starts to diminish, indicating a limit on peak attainable damping. The initial potential energy stored in the system (E_o) increases with θ_o. Since $\varepsilon \propto E_o$ [equation (7)], it also increases with θ_o [Figure 6(b)]. The energy dissipation plot also showed a similar trend.

3.3. Damper with an Obstacle

Experiments were carried out for a family of obstacles ($r = 6$–22 mm, $0{\cdot}0162 \leq r/L \leq 0{\cdot}0595$). Two obstacles were located symmetrically about the damper centerline ($d/L = 0{\cdot}25$) as shown in Figure 1. Figure 7 shows the performance of the damper as a function of h_w for various r/L ratios. The plot for $r/L = 0$ indicates results in the absence of

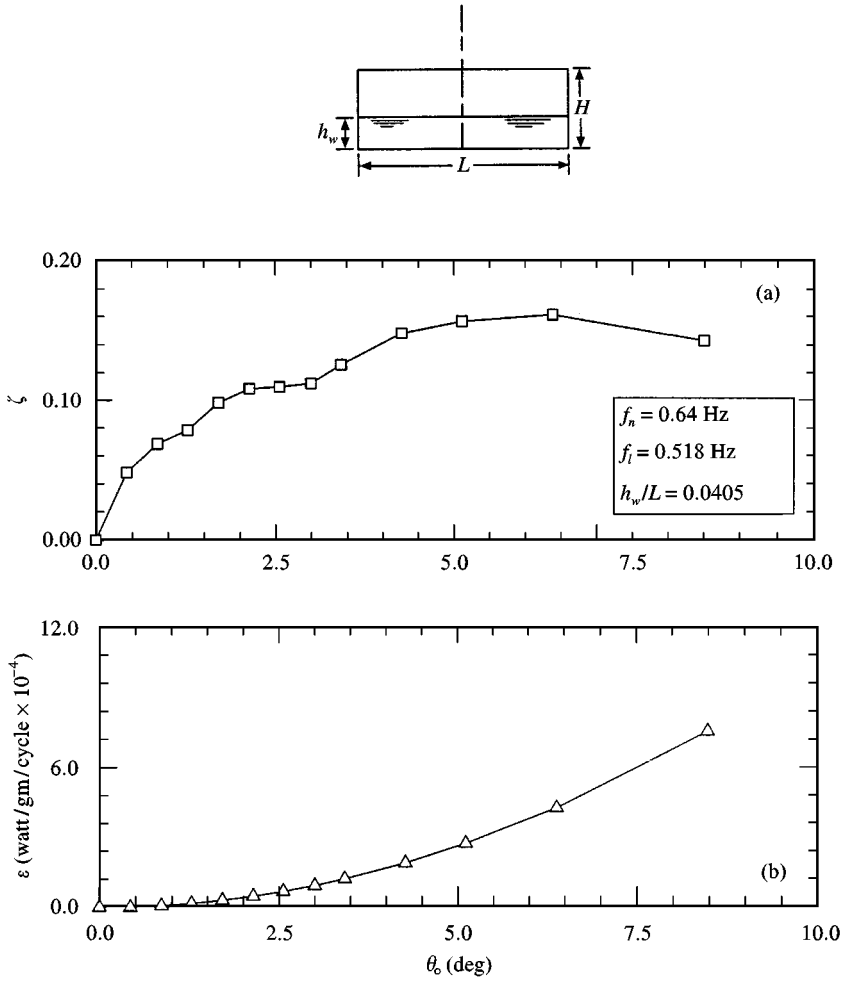

Figure 6. Performance of the liquid damper as affected by the initial displacement (θ_0).

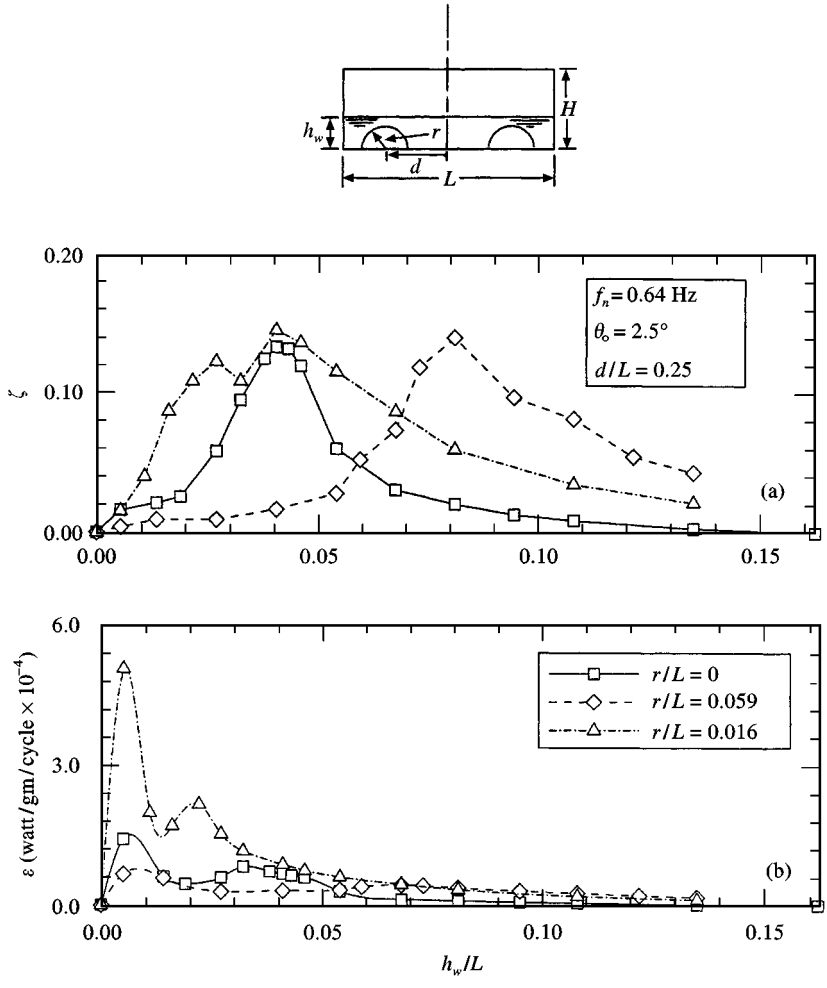

Figure 7. Performance of the liquid damper as affected by the liquid height (h_w) and the obstacle size.

an obstacle. For $r/L = 0$, there is a relatively sharp peak in the ζ versus h_w/L curve. In comparison, for $r/L = 0{\cdot}0162$, the peak in ζ extends over a wider range of liquid heights. The peak in ζ for $r/L = 0{\cdot}0595$ is shifted to the right and occurs at a much higher liquid height. The peak value of ζ remains essentially unaffected by the presence of an obstacle. The more important energy dissipation parameter, ε, provides a better picture. Note, there is a significant improvement in the damper performance with an obstacle of $r/L = 0{\cdot}0162$. Similar results were also obtained for $r/L = 0{\cdot}0297$ and $0{\cdot}0405$. From the above experiments, an obstacle with $r/L = 0{\cdot}0162$ (i.e. $r = 6$ mm) with $h_w/L = 0{\cdot}0216$ ($h_w = 8$ mm) appears quite promising.

Once the optimum obstacle size was determined, the next logical step was to determine the effect of its location (d) on the performance. Experiments were carried out for $0 \leq d/L \leq 0{\cdot}5$. Note, $d/L = 0$ means a single obstacle in the middle of the damper, whereas $d/L \approx 0{\cdot}5$ indicates obstacles touching the walls of the damper. As shown in Figure 8, ε does not appear to be sensitive to d/L. It is slightly higher for $d/L = 0$. Similar experiments with different r/L confirmed this observation.

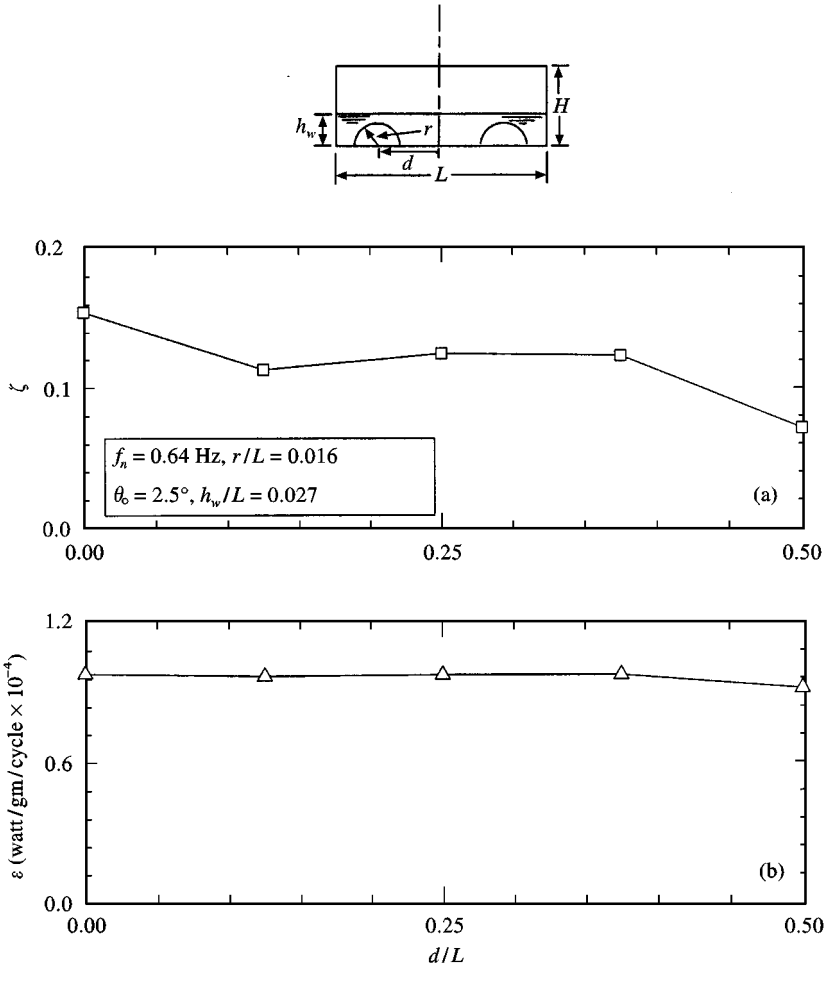

Figure 8. Effect of the obstacle location on the performance of the liquid damper.

Figure 9 shows the effect of the initial displacement (θ_o) on the performance of the optimal damper. As expected, ζ reaches a peak value and then begins to diminish. There is a significant improvement in the energy dissipation for the optimal damper. Of course, like ζ, it will eventually reach a peak and then decline at a sufficiently large θ_o.

4. SUPPRESSION OF FLOW-INDUCED INSTABILITIES

The parametric study of the damper was complemented with a wind tunnel test-program to evaluate the performance of liquid dampers in regulating both vortex resonance and galloping type of instabilities. A two-dimensional circular cylindrical model was used during the vortex resonance study while a two-dimensional square prism was employed during the galloping tests.

The experiments were carried out in a low-speed, low turbulence, closed-circuit wind tunnel, having a test-section of 0·68 m × 0·91 m. A light balsa wood model, supporting a damper at the top, was mounted in a specially designed dynamic test-rig which held a set

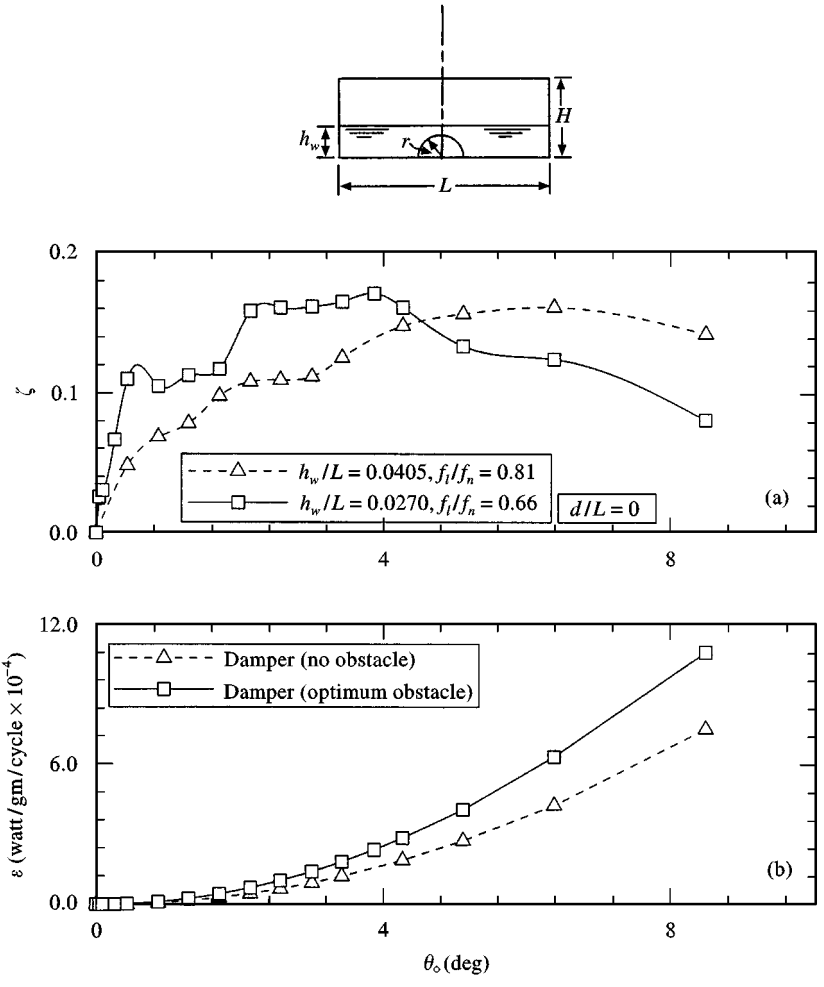

Figure 9. Performance of the liquid damper with and without an obstacle as affected by the initial displacement (θ_0).

of four air-bearings, a displacement transducer, as well as springs to impart desired stiffness to the model. The model was free to vibrate transverse to the flow direction (Figure 10). The damper used for the tests was a scaled-down replica ($L = 123$ mm; $W = 52$ mm; and $H = 45$ mm) of the one used for the free-vibration tests. The obstacle size and location were $r = 6$ mm and $d = 0$, respectively ($r/L = 0{\cdot}0488$). Typical results are presented in Figure 11.

Vortex resonance response of the circular cylinder is shown in Figure 11(a). In the absence of the liquid damper, the classical resonance peak with an amplitude of $y/D \approx 0{\cdot}086$ is apparent. With the liquid damper but in the absence of the obstacle, the peak response is around 0·042, a reduction of around 51%. The damper with the obstacle further improves the performance by approximately 18%. It is important to recognize that the liquid mass ratio is only 0·5%. Furthermore, the damper is purposely tested under a rather adverese condition, as f_l/f_n is taken to be 0·175 (rather than around 1)%, f_n is also much higher than 1 ($f_n = 2{\cdot}7$ Hz) where liquid dampers are known to be less efficient.

Figure 11(b) presents results of the galloping response of the square prism. In the absence of the damper, the model attains a large amplitude motion limited by the test arrangement

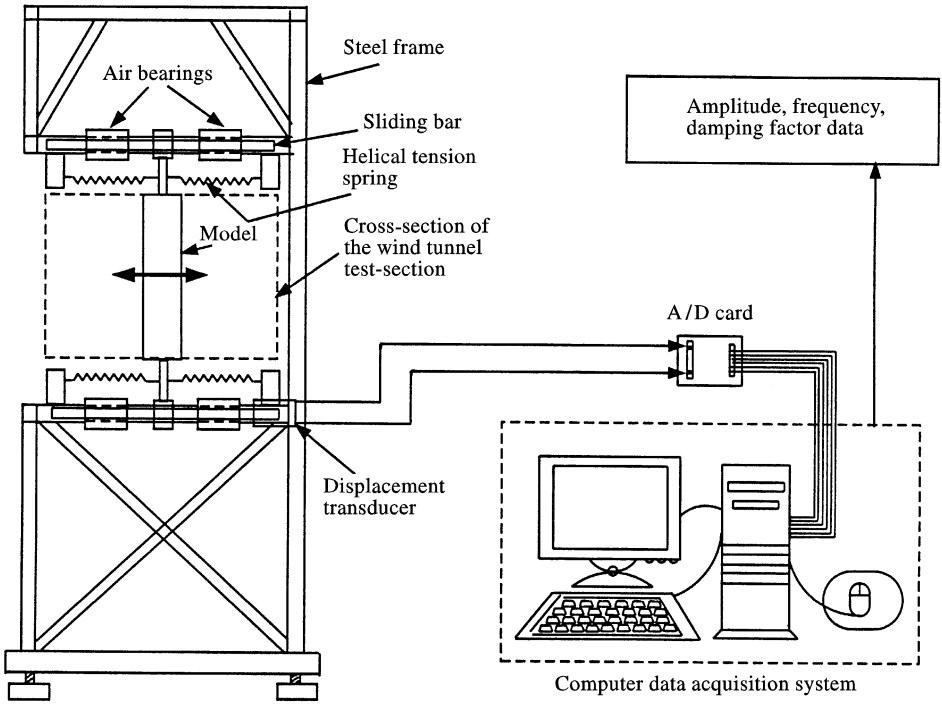

Figure 10. A schematic diagram of the dynamic experiment set-up involving the wind tunnel, test-rig and data acquisition system.

($y/D \approx 0{\cdot}3$). With the liquid damper but without the obstacle, the limit-cycle amplitude reduces by approximately 33%. However, with the damper modified with the obstacle, y/D is only 0·035, a reduction of 88%. Of course, by providing additional liquid to dissipate more energy and proper tuning, one can improve the performance further.

5. CONCLUDING REMARKS

Based on the parametric study with rectangular sloshing liquid dampers in presence of semi-circular obstacles and wind tunnel tests, the following general observations can be made.

(i) The results suggest a significant increase, up to 60%, in the energy dissipation capacity of the liquid sloshing damper by introduction of an optimum obstacle in the path of the moving liquid.

(ii) The presence of an obstacle leads to a wider peak, i.e., to higher damping over an extended range of liquid frequencies.

(iii) As expected, the performance of the damper depends on both the frequency ratio (f_n/f_l) and initial displacement (θ_o). There are optimum values for both.

(iv) The parametric study successfully identifies the optimum size and location of the obstacle as $r/L = 0{\cdot}016$ and $d/L = 0$ (i.e., one obstacle).

(v) Wind tunnel results suggest that with the improved damper design it is possible to regulate both vortex resonance and galloping type of fluid–structure interaction instabilities, even with a mass ratio (μ) of 1% or less. The presence of the obstacle significantly

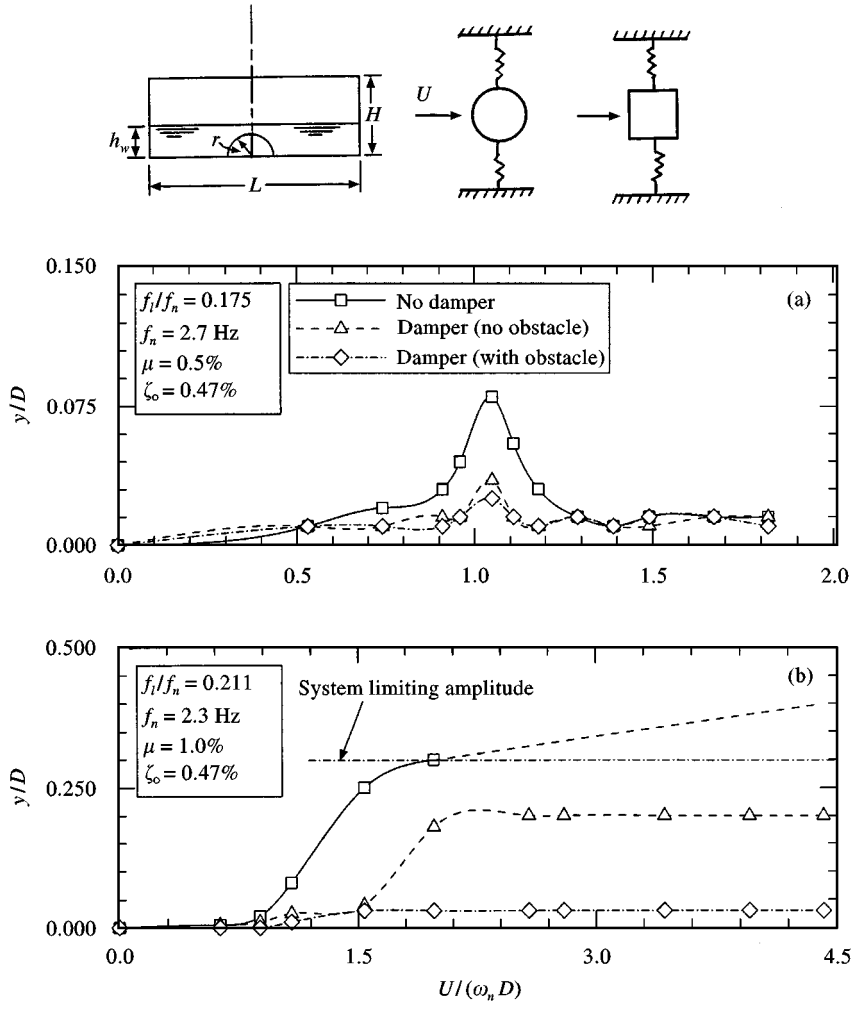

Figure 11. Control of flow-induced instabilities using the liquid sloshing damper: (a) vortex-induced vibrations experienced by a circular cylinder; (b) galloping response of a square-section prism.

improves the damper performance. During galloping, a further reduction in vibration amplitude in the presence of the obstacle by 55% is indeed remarkable.

(vi) The damper remains effective in controlling vibrations even under off-design conditions ($f_l/f_n = 0{\cdot}17$–$0{\cdot}21$, rather than 1).

(vii) Based on the parametric study as well as dynamic experiments in the wind tunnel, it can be said that the introduction of an optimum obstacle substantially increases the energy dissipation of a liquid damper and thereby primises to reduce the mass ratio (μ) necessary for vibration control of real-life structures.

ACKNOWLEDGEMENT

The investigation reported here was supported by the Natural Sciences and Engineering Research Council of Canada, Grant No. A-2181.

References

Abiru, H., Fujishiro, M., Matsumoto, T. & Nagata, N. 1992 Tuned active dampers installed in the Yokohama Landmark Tower. *Proceedings of the 1st International Conference on Motion and Vibration Control*, (eds K. Seto, K. Yoshida, K. Nonami), pp. 110–115 The Japan Society of Mechanical Engineers.

Alfriend, K. T. & Spencer, T. 1981 Comparison of filled and partly filled nutation dampers. *AAS/AIAA Astrodynamics Specialist Conference*, Lake Tahoe, Nevada, U.S.A., Paper 81–141.

Banning, D. A., Hengeveld, L. D. & Modi, V. J. 1966 Apparatus for demonstrating dynamics of sloshing liquids. *Bulletin of Mechanical Engineering Education* **5,** 65–70.

Blevins, R. D. 1979 *Formulas for Natural Frequencies and Mode Shape*, pp. 364–385. New York: Van Nostrand Reinhold.

Forbes, L. K. 1988 Critical free-surface flow over a semi-circular obstruction. *Journal of Engineering Mathematics* **22,** 3–13.

Fujino, Y. & Abe, M. 1992 Dynamic characterization of multiple tuned mass dampers. *Proceedings of the 1st International Conference on Motion and Vibration Control* (eds. K. Seto, K. Yoshida, K. Nonami) pp. 176–181. The Japan Society of Mechanical Engineers.

Hirsch, G. 1980 Control of wind-induced vibrations of civil engineering structures. *Proceedings of the 4th Colloquium on Industrial Aerodynamics*, (eds C. Kramer, H. J. Gerhardt, H. Ruscheweyeh and G. Hirsch), Part 2, pp. 237–256. Fluid Mechanics Laboratory, Department of Aeronautics, Fachhochschule, Aachen.

Irwin, P. A., Ferraro, V. & Stone, G. K. 1988 Wind induced motions of buildings. *Proceedings of the Symposium/Workshop on Serviceability of Buildings* (*Movements*, *Deformations*, *Vibrations*), Vol. I, pp. 200–213. National Research Council of Canada, Ottawa, Canada.

Kazao, Y., Takahara, K., Yamada, M. & Sakamoto, S. 1992 Active Vibration Control of a Structure Using Gyrostabilizer. *Proceedings of the 1st International Conference on Motion and Vibration Control* (eds K. Seto, K. Yoshida, K. Nonami), pp. 158–163. The Japan Society of Mechanical Engieers.

Kwok, K. C. S. 1991 Damping and control of structures subjected to dynamic loading. *Structures Subjected to Dynamic Loading – Stability and Strength* (eds R. Narayanan, T. M. Roberts), pp. 303–334. London: Elsevier Applied Science.

Masciantonio, A., Isyumov, N. & Petersen 1987 Wind-induced response of a tall building and comparisons with wind tunnel predictions. *Proceedings of the 6th Annual ASCE Structures Congress*, pp. 810–825. Orlando, U.S.A.

Mironer, A. 1979 *Engineering Fluid Mechanics*, pp. 463–475. New York: McGraw-Hill.

Modi, V. J., Sun, J. L. C., Shupe, L. S. & Solyomvari, A. S. 1981 Suppression of wind-induced instabilities using nutation dampers. *Proceedings of Indian Academy of Science* (*Engineering Science*) **4,** pp. 461–470.

Modi, V. J. & Welt, F. 1985 On the control of instabilities of fluid–structure interaction problems. *Proceedings of the 2nd International Symposium on Structural Control* (ed. H. H. E. Leipholz), pp. 473–486. Rotterdam: Martinus Nijhoff.

Modi, V. J. & Seto, M. L. 1995 On the energy dissipation through liquid sloshing and suppression of wind induced instabilities. *Proceedings of the 9th International Conference on Wind Engineering* **IV,** pp. 1619–1630. New Delhi: Wiley Eastern Limited.

Modi, V. J., Welt, F. & Seto, M. L. 1995 Control of wind induced instabilities through application of nutation dampers: a brief overview. *Journal of Engineering Structures* **17,** 626–638.

Munshi, S. R., Modi, V. J. & Yokomizo, T. 1995 Drag reduction and vibration suppression of a D-section structural member through momentum injection. *International Journal of Offshore and Polar Engineering* **5,** 161–165.

Ruschweyeh, H. 1980 Straked in-line steel stacks with low mass damping parameter. *Proceedings of the 4th Colloquium on Industrial Aerodynamics* (eds C. Kramer, H. J. Gerhardt, H. Ruscheweyeh and G. Hirsch) Part 2, pp. 185–204. Fluid Mechanics Laboratory, Department of Aeronautics, Fachhochschule, Aachen.

Schneider, C. C. & Likins, P. W. 1973 Nutation damper versus precession dampers for axisymmetric spinning spacecraft. *Journal of Spacecraft and Rockets* **10,** 218–222.

Seto, K. 1992 Trends on active vibration control in Japan. *Proceedings of the 1st International Conference on Motion and Vibration Control*, (eds. K. Seto, K. Yoshida, K. Nonami), pp. 1–11. The Japan Society of Mechanical Engineers.

Sorensen, R. M. 1978 *Coastal Engineering*, pp. 14–16. New York: Wiley.

TAMURA, Y., FUJII, K., SATO, T., WAKAHARA, T. & KOSUGI, M. 1988 Wind-induced vibration of tall towers and practical application of tuned sloshing damper. *Proceedings of the Symposium/Workshop on Serviceability of Buildings* (*Movements, Deformations, Vibrations*) Vol. I, pp. 228–241. National Research Council of Canada, Ottawa Canada.

TAMURA, Y., KOUSAKA, R. & MODI, V. J. 1992 Practical application of nutation damper for suppressing wind-induced vibrations of airport towers. *Journal of Wind Engineering and Industrial Aerodynamics* **41–44,** 1919–1930.

WELT, F. & MODI, V. J. 1992 Vibration damping through liquid sloshing: Part I – a nonlinear analysis. *ASME Journal of Vibration and Acoustics* **114,** 10–16.

WELT, F. & MODI, V. J. 1992 Vibration damping through liquid sloshing: Part II – experimental results. *ASME Journal of Vibration and Acoustics* **114,** 17–23.

ZDRAVKOVICH, M. M. 1981 Review and classification of various aerodynamic and hydrodynamic means for suppressing vortex shedding. *Journal of Wind Engineering and Industrial Aerodynamics* **7,** 145–189.

APPENDIX: NOMENCLATURE

A_0	initial vibration amplitude
A_n	amplitude of the vibration after n cycles
D	projected width of a bluff body normal to the flow
E_0	initial potential energy stored in the vibrating system, $\frac{1}{2}kA_0^2$
E_n	potential energy stored in the vibrating system after n cycles, $\frac{1}{2}kA_n^2$
F_1, F_2	Froude numbers based on depths z_1 and z_2 of the liquid, respectively
H	height of the rectangular damper
L	length of the rectangular damper
P_{atm}	atmospheric pressure
T	period of the vibrating system, f_n^{-1}
U	freestream velocity
V_1, V_2	liquid velocity upstream and downstream of an obstacle, respectively
W	width of the rectangular damper
c	phase velocity of the free surface waves, $\sqrt{gh_w}$
d	distance of the obstacle from the damper centreline
f_l	frequency of free surface waves in the liquid $\sqrt{gh_w}/(2L)$
f_n	natural frequency of the vibrating system
f_v	frequency of vortex shedding
g	gravitational acceleration
h_w	liquid height
k	stiffness
l	height of the liquid free surface measured with respect to the bearing support
m_l	liquid mass
n	number of vibration cycles
r	radius of the semicircular obstacle
y	amplitude (transverse to the flow direction) of an oscillating bluff body
z_1, z_2	liquid heights upstream and downstream of an obstacle, respectively
ε	energy dissipation parameter
δ	logarithmic decrement
ζ	damping factor due to liquid sloshing
ζ_0	inherent damping factor of the system in absence of the liquid damper
θ_0	initial angular displacement given to the vibrating system
λ	shallow water wavelength of the free surface waves in a rectangular container, $2L$
μ	mass ratio, ratio of the liquid mass to the structure mass
ω_n	circular natural frequency, $2\pi f_n$